Variability of Distribution of Ca2+/Calmodulin-Dependent Kinase II at Mixed Synapses on the Mauthner Cell: Colocalization and Association with Connexin 35

Article *in* The Journal of Neuroscience : The Official Journal of the Society for Neuroscience · July 2010

DOI: 10.1523/JNEUROSCI.4466-09.2010 · Source: PubMed

CITATIONS
27

READS
98

6 authors, including:

Carmen E. Flores Nakandakare
Lausanne University Hospital
15 PUBLICATIONS **669** CITATIONS
SEE PROFILE

Roger Cachope
CHDI Foundation
28 PUBLICATIONS **1,103** CITATIONS
SEE PROFILE

Srikant Nannapaneni
Maimonides Medical Center
8 PUBLICATIONS **201** CITATIONS
SEE PROFILE

Alberto E Pereda
Albert Einstein College of Medicine
66 PUBLICATIONS **2,265** CITATIONS
SEE PROFILE

Published in final edited form as:
J Neurosci. 2010 July 14; 30(28): 9488–9499. doi:10.1523/JNEUROSCI.4466-09.2010.

Variability of distribution of Ca^{++}/calmodulin-dependent kinase II at mixed synapses on the Mauthner cell: co-localization and association with connexin 35

Carmen E. Flores[1], **Roger Cachope**[1], **Srikant Nannapaneni**[1], **Smaranda Ene**[1], **Angus C. Nairn**[2], and **Alberto E. Pereda**[1,*]

[1] Dominick P. Purpura Department of Neuroscience, Albert Einstein College of Medicine, Bronx, New York

[2] Department of Psychiatry, Yale University, New Haven, Connecticut

Abstract

In contrast to chemical transmission, few proteins have been shown associated with gap junction-mediated electrical synapses. Mixed (electrical and glutamatergic) synaptic terminals on the teleost Mauthner cell known as “Club endings” constitute because of their unusual large size and presence of connexin 35 (Cx35), ortholog of the widespread mammalian Cx36, a valuable model for the study of electrical transmission. Remarkably, both components of their mixed synaptic response undergo activity-dependent potentiation. Changes in electrical transmission result from interactions with co-localized glutamatergic synapses, the activity of which leads to the activation of Ca^{++}/calmodulin-dependent kinase II (CaM-KII), required for the induction of changes in both forms of transmission. However, the distribution of this kinase and potential localization to electrical synapses remains undetermined. Taking advantage of the unparalleled experimental accessibility of Club endings, we explored the presence and intraterminal distribution of CaM-KII within these terminals. Here we show: 1) unlike other proteins, both CaM-KII labeling and distribution were highly variable between contiguous contacts, and 2) CaM-KII was not restricted to the periphery of the terminals, where glutamatergic synapses are located, but also was present at the center where gap junctions predominate. Accordingly, double-immunolabeling indicated that Cx35 and CaM-KII were co-localized and biochemical analysis showed that these proteins associate. Because CaM-KII characteristically undergoes activity-dependent translocation, the observed variability of labeling likely reflects physiological differences between electrical synapses of contiguous Club endings, which remarkably co-exist with differing degrees of conductance. Taken together, our results indicate that CaM-KII should be considered a component of electrical synapses although its association is non-obligatory and likely driven by activity.

Keywords

Electrical synapse; LTP; connexin 36; gap junction; synaptic plasticity; auditory afferent

INTRODUCTION

As a result of their unusually large size (~10 μm), a group of contacts on the lateral dendrite of the teleost Mauthner (M−) cells has provided since their discovery (Bartelmez, 1915) the

*Correspondence should be addressed to: A.E. Pereda, Dominick P. Purpura Department of Neuroscience, Albert Einstein College of Medicine, 1300 Morris Park Ave., Bronx, NY 10461. Phone: (718) 430 3405. Fax: (718) 430 8821. alberto.pereda@einstein.yu.edu.

opportunity of examining diverse structural features of vertebrate synapses. These “striking synapses” are terminations of auditory afferents originating in the anterior part of the sacculus, and are known as “Large Myelinated Club endings” (Club endings; CEs) (Bartelmez, 1915). Studies on CEs provided early evidence for the lack of protoplasmatic continuity between pre- and postsynaptic elements (Bartelmez and Hoerr, 1933) and, with the advent of electron microscopy, with early evidence for the structural basis of electrical transmission: the gap junction (Robertson et al., 1963). Ultrastructural (Tuttle, et al., 1987) and confocal microscopy (Pereda et al., 2003) studies show that while gap junctions (up to ~200) are distributed throughout the surface of the contact, chemical synapses are predominantly restricted to the periphery (Tuttle, et al., 1987). Thus, the large size of these terminals and differential segregation of the structural components for both forms of transmission makes them amenable for exploring the presence and detailed sub-cellular distribution of various proteins associated to these modalities of synaptic transmission.

The physiological features of CEs can also be easily explored, allowing the uncommon correlation between synaptic structure and function (for review see Pereda et al., 2004). Consistent with the co-existence of gap junctions and chemical synapses at these terminals (“mixed synapses”), electrical stimulation of saccular afferents evokes a mixed, electrical and chemical, synaptic potential in the lateral dendrite of the M-cell (Furshpan, 1964; Lin and Faber, 1988a). While chemical transmission is mediated by glutamate (Wolszon et al., 1997), gap junctions contain connexin 35 (Cx35) (Pereda et al., 2003) the fish ortholog of the neuronal connexin 36 (Cx36), which is widely expressed throughout mammalian brain (Condorelli et al., 1998). Strikingly, both components of the mixed synaptic response undergo activity-dependent potentiation of their respective strengths (Yang et al., 1991; Pereda and Faber, 1996). Thus, changes are not restricted to chemical synapses but also involve the regulation of gap junction-mediated electrical synapses. The mechanism underlying modifications in electrical transmission reflects a functional interaction with neighboring co-localized glutamatergic synapses, where activity leads to the activation of the multifunctional Ca^{++}/calmodulin-dependent kinase II (CaM-KII), necessary for the induction of changes in both forms of transmission (Pereda et al., 1998). Yet, the distribution and relationship of CaM-KII to chemical and electrical synapses within CEs remains undetermined.

CaM-KII has been implicated in mechanisms of activity-dependent plasticity in chemical synapses (Fink and Meyer, 2002; Schulman 2004; Merill et al., 2005; Wayman et al., 2008). This kinase is an essential and abundant component of glutamatergic postsynaptic densities (PSDs) (Kennedy, 2000) where it associates with other proteins, such as NMDA receptors (Yang and Schulman, 1999; Strack et al., 2000). Recent data indicate that this kinase can also molecularly interact with Cx36 (Alev et al., 2008). Together with the well-established functional role of CaM-KII in CEs (Pereda et al., 1998), the high homology of Cx36 with its fish ortholog suggests a potential association of this kinase with Cx35 at these terminals. Moreover, the dynamic spatial properties of CaM-KII which are based on its ability to translocate to active synapses (Shen and Meyer, 1999; Merill et al., 2005; Rose et al., 2009; Lee et al., 2009), including in fish (Gleason in al., 2003), suggest that its intraterminal distribution could reflect its functional role in these terminals.

To investigate the distribution of CaM-KII in CEs, we took advantage of the unique experimental accessibility of the M-cell system for imaging single synaptic terminals using confocal microscopy. Here we show that, the distribution of CaM-KII was highly variable between contiguous CEs. Furthermore, CaM-KII was found not only in the periphery of the terminals, where glutamatergic PSDs are located, but also at the center where gap junctions predominate. Double-immunolabeling and biochemical approaches showed that Cx35 and CaM-KII associate, indicating that these proteins functionally interact at electrical synapses in

CEs. We speculate the observed heterogeneinity of labeling may reflect differences in functional states between adjacent CEs.

MATERIAL AND METHODS

Immunocytochemistry

Goldfish (*Carassius auratus*) 2–5" long were perfused with phosphate buffered saline (1X PBS) at pH 7.4 for 10–15 min followed by cold 4% paraformaldehyde in 0.1 M phosphate buffer for 10–15 min. Brains were dissected out and kept overnight at 4°C in 4% paraformaldehyde in 0.1 M phosphate buffer. Brains were sectioned (40–50 μm) with a TPI microtome (Vibratome, Technical Products International). The sections were rinsed at room temperature three times for 10 min each with 1X PBS, blocked and permeabilized for 45 min to 1 h at room temperature in PBStr (1X PBS, 0.3–0.4% Triton X-100, pH 7.4) plus 10% normal goat serum (NGS). Sections were incubated overnight at 4°C using a moving platform with rabbit polyclonal G301 anti-αCaM-KII (1:1000) and/or mouse monoclonal anti-Cx35/36 (Chemicon; 1:250/500). A previously characterized teleost anti-NR1 antibody directed against the NR1 subunit of the electric fish *Apteronotus* (Berman et al., 2001; gift of Drs. L. Maler and R. Dunn) was used as a marker for glutamatergic synapses. Then, sections were rinsed in PBStr four times for 10 min each wash and incubated for 1–2 h at room temperature with Alexa Fluor 594-conjugated goat anti-rabbit and Alexa Fluor 488-conjugated goat anti-mouse (Molecular Probes; 1/500) or Texas Red goat anti-rabbit (Jackson ImmunoResearch; 1/500) or FITC goat anti-mouse (Chemicon; 1/250) secondary antibodies. Finally, sections were rinsed with PBStr three times for 10 min each wash and then 10 min with 50 mM phosphate buffer, pH 7.4, and mounted on slides in a propyl gallate-based antifading solution to reduce photobleaching. Control sections were routinely incubated with secondary antibodies in the absence of primary antibodies.

Confocal microscopy and image processing

Sections were imaged with an Olympus BX61WI confocal microscope with a mortised fixed stage with 20X air, 40X apo/340 water, and 60X oil objective lenses. FLUOVIEW FV500 software was used for data acquisition. XY images were scanned in the z axis at 0.5–0.8 μm intervals for 3D reconstruction. Z-plane sections and Z-plane stacks were analyzed using Image J software (National Institutes of Health). For presentation purposes, some images were processed with Adobe Photoshop (Adobe Systems) and Canvas X (ACD Systems). For the analysis of CaM-KII labeling, 8 bit images of individual CEs were background-subtracted and thresholded using Image J to include signals at least 1.5- to 2-fold greater than the background signal. Regions of interest corresponding to the surface area of individual CEs were identified using differential interference contrast (DIC) microscopy and/or Cx35 labeling during double-labeling experiments. To investigate its distribution at CEs, CaM-KII labeling at two concentric, peripheral and central, areas of each CE (considered for this purpose as an ellipse; Fig.4D) were quantified using Image J (Fig.4D). These areas represented 36% and 49% of the total surface of the terminal, respectively. A transition ring between these two regions (15%) was not taken into account (Fig.4D) to better contrast the distribution of labeling between these areas. The rationale behind this analysis was that while CaM-KII is expected to be present in the periphery of the terminals where the majority of the glutamatergic PSDs are located, its localization in the center would be suggestive of its association to gap junctions, which predominate in this area. To illustrate the variability in the distribution of CaM-KII labeling within the population of CEs we used a ratio between labeling at central and peripheral areas. This index was defined as: *"Periphery-Center Index" = Labeling Center − Labeling Periphery / Labeling Center + Labeling Periphery, where "Labeling Center" = Σ (labeling Intensity above threshold at Center * number of pixels) / Center area, and "Labeling Periphery" = Σ (labeling Intensity above threshold at Periphery * number of pixels) / Periphery*

area. Indices approximating −1 indicate prevalence of labeling at the periphery of the CE, whereas those approximating +1 indicate prevalence of labeling at the center. Finally, indices approximating 0 are indicative of a comparable labeling between center and periphery. For presentation purposes, some images were processed using Adobe Photoshop (Adobe Systems, San Jose, CA) and Canvas X (ACD Systems). For colocalization analysis, images of individual CEs were background subtracted and thresholded to include signals that were at least 2–3 fold greater than the scatter labeling at the dendrite. Regions of interest corresponding to individual CEs were identified in Metamorph using transmitted light images and Cx35 labeling. Co-localization was measured as the percentage of the area labeled for one channel that was also labeled for the second channel and the converse.

Co-Immunoprecipitation

Fresh tissue samples of ~90 mg and containing both M-cells, as well other smaller reticulo- and vestibulospinal neurons, were obtained from goldfish hindbrain ventral to the cerebellum and between rostral and caudal margins of the cerebellar peduncles. Samples were rapidly stored at −80°C until homogenization. At 4°C, IP buffer (20 mM TRIS-HCl, pH 8.0, 140 mM NaCl, 1% Triton X-100, 10% glycerol, 1 mM EGTA, 1.5 mM MgCl2, 1 mM dithiothreitol, 1 mM phenylmethylsulfonyl fluoride (PMSF), 5 μg/ml of the protease inhibitors leupeptin, pepstatin A, and aprotinin) were added to the thawed samples for homogenization. Homogenates were sonicated at 4°C 3 times for 10 s each, 35% duty cycle with a W-225R sonicator (Misonix, Inc) and centrifuged for 10 min at 14,000 × g at 4°C, and the supernatant was collected for further analysis (Western blotting and co-immunoprecipitation). Protein was quantified using BCATM Protein Assay Kit (Pierce). Aliquots of supernatants (2 mg protein) were pre-cleared for 1 h at 4°C using 30 μl protein A-coated agarose beads (Santa Cruz BioTech, Santa Cruz, CA, USA) and centrifuged at 14,000 g for 10 min at 4°C. Supernatants were incubated with 2 μg of G301 rabbit anti-αCaM-KII antibody overnight at 4°C on a moving platform, followed by 1 h incubation with 30 μl protein A-coated agarose beads. The mix was then centrifuged as above for 10 min at 4°C. The pellets were washed five times with 500 μl-1 ml of wash buffer (20 mM TRIS-HCl, pH 8.0, 150 mM NaCl, 0.5% NP-40) and incubated at 60°C for 2 min in SDS-PAGE loading buffer containing 5–10% β-mercaptoethanol. Samples were resolved on 10% or 12% SDS-PAGE gels. Proteins were transferred at 30V overnight to nitrocellulose membranes (Schleicher and Schuell, Germany) in standard tris-glycine transfer buffer (pH 8.3) containing 0.5% sodium dodecylsulphate. In order to confirm transfer efficiency, membranes were stained with Ponceau-S (Sigma, USA). Blots were blocked for 1–3 h at room temperature with 4–5% nonfat dry milk in TSTw (20 mM Tris-HCl, pH 7.4, 150 mM NaCl, 0.1% Tween 20), rinsed briefly in TSTw, and then incubated overnight at 4°C using a moving platform with mouse anti-Cx35/36 (2 μg/ml) or mouse anti-ZO-1 (2–3 μg/ml) antibodies. Antibodies were diluted in TSTw containing 1% nonfat dry milk. Membranes were washed with TSTw 3 times for 10 min., incubated for 1 h with horseradish peroxidase-conjugated goat anti-mouse IgG (Santa Cruz biotechnology, USA, diluted 1:7500), washed with TSTw 4 times for 10 min and once for 10 min with 20 mM TRIS-HCL, pH 8.0. Proteins were then resolved by chemiluminescence ECL (Amersham Biosciences, USA). Control samples were precipitated in the absence of CaM-KII antibody.

Electrophysiology and dye coupling

Surgical and recording techniques were similar to those described previously (Smith and Pereda, 2003; Curti and Pereda, 2004). Briefly, individual VIIIth nerve afferents were sequentially penetrated outside the brain (electrodes contained 2.5 M KCl; 35–45 MΩ) while a second electrode (5 M KAc, 4–12 MΩ) was kept inserted in the M-cell lateral dendrite, 350–400 μm from the axon cap of the cell. Afferents with electrical synapses on the M-cell were identified by the presence of electrotonic coupling potentials when the M-cell antidromic spike was evoked by stimulating the spinal cord (Furshpan, 1964; Lin and Faber, 1988a; Smith and

Pereda, 2003; Curti and Pereda, 2004). The resting potential of the afferents and the M-cell averaged 71 mV (±05 mV S.E.M., n=140) and 78.7 mV (±2.5 mV S.E.M., n=95), respectively. Only, afferents with resting potentials of at least −60 mV were used for the analysis. For dye coupling evaluation, the M-cell was recorded intracellularly with electrodes containing a 4% solution of Neurobiotin (MW: 322.8) in 2.5 M KCl and this solution was iontophoretically-injected (400 ms pulses of 50 nA for 20 min), visualized with Avidin-conjugated DAB and examined under transmitted light microscopy. To avoid unintentional extracellular leakage of Neurobiotin around the CEs, the injections were performed in the soma, which is about 400 μm from the CEs terminal field. After injections, waiting periods of 1 to 2 h were used to allow diffusion of the dye (for details see Smith and Pereda, 2003). Coupling coefficients for individual CEs were estimated as the ratio between the amplitude of the electrical component (or coupling potential) of the unitary synaptic potential and the amplitude of the presynaptic spike (coupling coefficient = coupling potential / presynaptic spike). This approximation is a convenient experimental advantage of the M-cell because: 1) the presynaptic action potential is an active signal of constant amplitude between Club endings afferents, and 2) the fast time constant of the M-cell dendrite, estimated in ~400 μs (Fukami et al., 1965), does not disproportionably attenuate fast voltage transients allowing reliable measurements of coupling. An average value of 88 mV (±1.09 mV S.E.M.; n=150) was used for the presynaptic spike amplitude, as the amplitude observed at the recording site at each might not be representative of its amplitude at the contact. The spike recorded at the site of depolarization regenerates in subsequent nodes and the presynaptic terminal (Lin and Faber 1988a; Smith and Pereda, 2003; Curti et al., 2008).

In-silico alignments and predictions of binding and phosphorylation sites

The amino acid sequence of the murine CaM-KIIα (NP_803126.1) regulatory site (Rosenberg et al., 2005) was aligned to its fish counterpart (zebrafish CaM-KIIα; UnitProKB:Q32PV2) and amino acid sequences of αCaM-KII binding and phosphorylation sites of mammalian Cx36 (gi|8928062) (Alev et al., 2008) were aligned to both perch Cx35 (gi|3420235) and Cx34.7 (gi|3420237) using EMBOS (EMBL-EBI, http://www.ebi.ac.uk/Tools/emboss/align/). In all cases, amino acid homology was expressed in terms of percentage of similarity, which takes into account identity as well conserved amino acid substitutions. Group-based Prediction System Version 2.1 (GPS *v*2.1) was used for prediction of αCaM-KII phosphorylation sites in mammalian Cx36 and perch Cx35 and Cx34.7, using a high threshold with a cutoff of 2.917. High threshold analysis has been validated by large scale predictions of mammalian phosphorylation sites (GPS 2.0; Xue et al., 2008). The cutoff values used in this analysis offered 98.5% accuracy, 100% sensitivity, 98.48% of specificity and 0.7117 Mathew correlation coefficient (MCC) and are were set on a calculated False Positive Rate (FPR) (GPS 2.0; Xue et al., 2008). The prediction of serine 293 as phosphorylation target site in Cx36 required a lower threshold (medium), which still offers high accuracy and sensitivity (90.71% accuracy, 100% sensitivity, 90.56% of specificity and 0.4673 MCC).

RESULTS

Identification of Club endings

The CEs represent the most recognizable input to the M-cells and originate from a population of about 90 saccular afferents that segregate to the distal portion of the lateral dendrite (Fig. 1A) (Bartelmez, 1915). Because of their unusually large size and high expression of Cx35, CEs can be unequivocally identified using antibodies that recognize Cx35 (Fig. 1B) (Pereda et al., 2003;Flores et al., 2008). As illustrated in Fig. 1B, the use of an anti-Cx35 monoclonal antibody (Cx35/36,Chemicon) characteristically yields intense punctate staining at the contact areas between CEs and M-cells (Fig. 1B–D). The number of anti-Cx35 fluorescent puncta observed at individual CEs is consistent with a previous ultrastructural demonstration of 63–

200 closely spaced gap junction plaques at individual CEs (Tuttle et al. 1983), suggesting that each punctum represents an individual plaque (Flores et al., 2008). The correspondence of this immunolabeling to CEs was confirmed in double–labeling experiments in which the saccular afferents were also labeled (Fig. 1B–D), where Cx35 labeling was found at the contact area of each afferent and the M-cell dendrite. These contacts were also easily identifiable on the surface of the lateral dendrite using differential interference contrast (DIC) microscopy (inset Fig. 1E). Additionally, this labeling pattern was confirmed using other anti-connexin antibodies (Pereda et al., 2003) and anti-zonula occludens-1 (ZO-1) antibodies (see below), a protein which exhibits a high-degree of co-localization with Cx35 (Flores et al., 2008).

Labeling for CaM-KII is highly variable between Club endings

In order to investigate the presence and distribution of CaM-KII at CEs, we performed immunofluorescence labeling using an antibody that exhibits relative selectivity for the αsubunit of rat brain CaM-KII (G-301, directed against a sequence in the autoregulatory domain of the rat brain α-subunit) and that we previously showed recognizes goldfish CaM-KII in western blots (Pereda et al., 1998). As previously reported, this antibody showed intense labeling of the M-cell (Fig.2A–B; Fig. 3B–C), which is consistent with the fact that CaM-KII interacts with proteins associated with cytoskeleton (Sahyou at al, 1985; Ohta et al., 1986). This distinct pattern constituted an internal control for the specificity of CaM-KII labeling. At the surface of the dendrite, this antibody labeled ovoidal structures that were reminiscent, because of the size and location, of CEs. The observed labeling matched that of CEs in double-labeling experiments using a Cx35 antibody (Fig.2C–D), and when visualizing these terminals with the help of DIC (not shown). Thus, our results indicate that CaM-KII can be detected at the areas of contacts between CEs and the M-cell.

Interestingly, in contrast to the predictable regularity of the labeling observed using the Cx35 antibody (Figs. 1B, 3A), the amount of labeling with the CaM-KII antibody was not constant but highly variable between contiguous CEs (Fig. 3B–C; Fig. 4C). Such variability of labeling was observed in all analyses of CaM-KII immunorectivity (n=5 fish). Furthermore, detailed examination of individual CEs using high-resolution confocal microscopy revealed that the spatial distribution of CaM-KII within the contact areas was also highly variable. While gap junctions are known to be distributed throughout the entire surface of the contact (Fig. 4A), glutamatergic synapses are primarily distributed in the periphery (Fig.4B), where PSDs are located (Tuttle et al., 1986). Such differential segregation makes CEs ideal for examining the relative distribution of diverse synaptic proteins to these co-existent modalities of transmission (see cartoon in Fig. 1A). We found that while CaM-KII labeling was predominant in the periphery, which is consistent with localization to glutamatergic PSDs (Fig. 2B), it was also unexpectedly found at the center of the contacts and, in some cases, distributed throughout their entire surface (Fig. 4C). In order to document and quantify the difference in the spatial distribution of CaM-KII, we expressed this variability as a ratio between the amount of labeling detected at the periphery and that detected at the center of the terminals (Fig. 4D). As illustrated in the summary graph (Fig. 4D), the estimated “Periphery/Center Index” (see Methods for details) was highly variable between CEs, indicating that the intraterminal distribution of CaM-KII is not a consistent feature at these contacts. Confirming such variability in its spatial distribution, the amount of CaM-KII labeling in both the total area and at the center of the contact were highly variable between CEs (Supp. Fig. 1A and 1B respectively). Furthermore, these two measurements were highly correlated (Supp. Fig. 1C), indicating that the amount detected at the center substantially contributes to the total amount of CaM-KII in CEs.

Association of CaM-KII with connexin 35

The unexpectedly variable spatial distribution of CaM-KII within CE terminals suggested that it could be associated with proteins other than those located at PSDs. In particular, the presence

of CaM-KII labeling in the center of the terminals suggests that CaM-KII could also associate with proteins at Cx35-containing gap junction plaques, which are highly predominant in this region of the contact (Tuttle et al., 1986). To investigate this possibility we looked for co-localization of Cx35 and CaM-KII in double labeling experiments (Fig. 5). We found a clear localization of CaM-KII at many Cx35-labeled puncta (Fig. 5A–B). The degree of co-localization of Cx35 with CaM-KII was lower in comparison to previous studies of co-localization of this connexin with the scaffold protein ZO-1 (see below), and it was highly variable between adjacent CEs. Averaged over individual endings, 66.7% (± 32.5, S.D.) of the area of Cx35 immunolabeling also showed CaM-KII labeling and, conversely, 70.1 % (± 18.6, S.D.) of the area of CaM-KII labeling also showed Cx35 labeling (n=28). As already mentioned above, the degree of colocalization was highly variable, ranging from 6.4% to 81% and 15.9% to 79% for Cx35 over CaM-KII and CaM-KII over Cx35, respectively. Strikingly, the variability of co-localization was found in immediately adjacent Cx35-labeled puncta, within the same region of a single contact (Fig. 5B). Because each punctum is thought to represent an individual gap junction plaque, such differential labeling of adjacent plaques indicates that the co-localization of Cx35 and CaM-KII might not be obligatory in nature and reflective of their functional interaction. Thus, its distribution to the center of the terminals might represent the extent of its functional association with Cx35 at gap junction plaques in CEs.

The co-localization of Cx35 and CaM-KII together with the high homology of this connexin with its mammalian ortholog Cx36 (O'Brien et al., 1998), which has been shown recently to interact with CaM-KII (Alev et al., 2008), suggested that these two proteins might also associate and interact in goldfish brain. To directly explore the possible association of Cx35 with CaM-KII, we first performed in-silico analysis of mammalian and teleost αCaM-KII sequences as well as of mouse Cx36 and perch Cx35 (see methods). Alignments of the mammalian and teleost sequences of the αCaM-KII regulatory region revealed that they are highly homologous (100% similarity in the pseudotarget and pseudosubstrate regions) (Supp. Fig. 2A), and that core amino acids for binding of the αCaM-KII autoregulatory region to αCaM-KII catalytic domain are conserved [Only one gene for αCaM-KII has been identified in teleost; ZFIN ZDB-GENE-051113–72]. Furthermore, sequence alignment of the described Cx36 cytoplasmic loop (CL) binding (pseudotarget) and carboxy terminus (CT) binding (pseudosubstrate) binding regions (Alev et al., 2008) showed that these areas were highly conserved in Cx35, with 86% and 92% similarity for the CT and CL regions, respectively (Fig. 5C and Supp. Fig. 2B). Similar results were obtained for Cx34.7, another perch Cx36 homolog (O'Brien et al., 1998), which showed 76.2% and 84% of similarity for the CT and CL regions, respectively (Supp. Fig. 2B), suggesting that CaM-KII association mechanisms are highly conserved and likely represent an important regulatory feature of neuronal connexins.

To investigate whether Cx35 and αCaM-KII associate in goldfish brain we performed co-immunoprecipitation studies using the G-301 antibody. This analysis was performed in samples obtained from a small area of the goldfish hindbrain containing the colossal M-cells, along with some other smaller reticulospinal and vestibulospinal neurons (see Supp.Fig.3 and Methods). Thus, this sample should be representative of the M-cell contents. αCaM-KII was immunoprecipitated from these hindbrain homogenates and immunoblots were probed with the Cx35 monoclonal antibody (Cx35/36, Chemicon). Immunoprecipitation of αCaM-KII resulted in the detection of a Cx35 band at the predicted molecular weight (Fig. 5D, lanes 2 and 3), which were comparable to migration profiles previously reported (Flores et al. 2008). While western blots detected a small presence of Cx35 (Fig. 5D, lane 1) in the input, more prominent bands were seen with the immunoprecipitation from two different samples (Fig. 5D, lanes 2 and 3), indicating that αCaM-KII more efficiently pulled-down this connexin as a result of their association. Interestingly, multiple bands were identified with the Cx35 antibody, suggesting the existence of multiple phosphorylation states of this connexin (Fig. 5D, lanes 2 and 3).

Recently, four αCaM-KII phosphorylation sites were described for Cx36 (Alev et al., 2008). In order to investigate the presence of putative phosphorylation sites forαCaM-KII in Cx35 we performed in-silico analysis using Group-based Prediction System version 2.1 (GPSv.2.1) software (see methods) in mouse Cx36, and perch Cx35 and Cx34.7 sequences. This analysis confirmed the presence of residues S110, T111, S277 and S315 in Cx36 as αCaM-KII targets. Five sites, S110, T111 both in the intracellular loop, and S128, S276 and S298 in the carboxy terminus were identified for Cx35 (Supp. Fig.4), where the last two correspond to sites S293 and S315 of Cx36, respectively. Residues S110 and S276 (S110 and S293 of Cx36) (Urschel et al., 2006) were previously described as PKA phosphorylation sites (Kothmann et al., 2007; O'Brien, 1998), suggesting that they are targets shared by both kinases. S298 (equivalent to S315 in Cx36) on the other hand seems to be exclusive for αCaM-KII. Only three putative sites were identified for Cx34.7: S110, S277 and S300, which correspond to residues S110, S276 and S298 of Cx35, and S110, S293 and S315 of Cx36, respectively. Thus, our *in-silico* analysis is consistent with the possibility of multiple phosphorylation states for Cx35.

Taken together, our *in-silico* and biochemical results suggest that CaM-KII associates with Cx35 in goldfish brain. Several proteins have been also shown to interact with connexins indicating the existence of protein complexes associated to gap junction channels (Herve et al., 2004). We have recently reported that ZO-1 extensively co-localizes and associates with Cx35 at CEs (Flores et al., 2008). In contrast to the less abundant and highly variable labeling of CaM-KII, ZO-1 was shown to extensively co-localize with Cx35 (85.53%, ± 14.45 S.D., of Cx35 colocalizes with ZO-1 labeling and 86.06%, ± 15.45 S.D., of ZO-1 colocalizes with Cx35, n=116; Flores et al., 2008) (Fig. 6A) and to directly interact with the last four aminoacids of its carboxy-terminus (Flores et al., 2008), suggesting that this scaffold protein might play a structural role in gap junction plaques at these terminals. Thus, we hypothesized that if CaM-KII directly interacts with Cx35, immunoprecipitation studies with the G-301 antibody should be also able to detect ZO-1. For this purpose, we performed co-immunoprecipitation studies in which CaM-KII was immunoprecipitated from hindbrain homogenates. In this case, immunoblots were probed with a monoclonal ZO-1 antibody, also used for immunolabeling of ZO-1. Immunoprecipitation of CaM-KII resulted in the detection of a ZO-1 band at the predicted molecular weight (Fig. 6B). These results suggest that CaM-KII associates with Cx35, and together with ZO-1, is likely to be part of the same macromolecular complex where channel-forming, scaffold and regulatory proteins coexist.

Variability of electrical coupling between contiguous terminals

While both sequence alignments and immunoprecipitation studies suggest that Cx35 and αCaM-KII interact at CEs, co-localization studies suggest that this association might not be obligatory, as variable labeling was found even between plaques within the same terminal. Because CaM-KII is known to translocate and aggregate to target sites following activity (Shen and Meyer, 1999; Merill et al., 2005; Rose et al., 2009; Gleason in al., 2003), its intraterminal distribution could be indicative of the degree of potentiation at individual CEs. Accordingly, the variability of CaM-KII labeling between immediately adjacent CEs was reminiscent of the variability of unitary electrical components of the mixed (electrical and chemical; Fig. 7A) synaptic potential evoked by stimulation of a single CE, which differ dramatically in amplitude (Smith and Pereda, 2003). To further demonstrate the extent and consistency of this phenomenon we compared the strength of electrical coupling between individual CE afferents and the M-cell lateral dendrite between different fish. For this purpose, we obtained multiple simultaneous pre- and postsynaptic recordings sequentially from individual CE afferents and the same M-cell lateral dendrite. As shown in Figure 7A where seven consecutive single terminals recordings are illustrated, the amplitude of the electrical components differed dramatically. [Characteristically, most CE single terminal recordings lack a chemical component (Lin and Faber, 1988b) and transmitter release is enhanced by co-activation of

multiple terminals (see Pereda et al., 2004)] This same variability was observed for five different fish in which unitary potentials were recorded in each M-cell dendrite during stimulation of 6–8 terminals (Fig.7C). Given that these single terminals originate from almost 90 large saccular afferents (Bodian, 1937), this sample represents approximately 8–10% of the total population of CEs in each lateral dendrite. In contrast to previous studies (Smith and Pereda, 2003), we expressed this variability in terms of coupling coefficients of orthodromic coupling produced by presynaptic action potentials (Fig. 7C), an estimate which is greatly facilitated by the fast time constant of the lateral dendrite of the M-cell (Fukami et al., 1965) (see methods). The properties of the presynaptic action potentials are highly constant across the population of CEs (Curti et al., 2008). Furthermore, because they were all recorded in the same postsynaptic cell (which makes corrections for differences in input resistance unnecessary), these coupling coefficients are highly correlated with the gap junctional conductance of individual terminals. The differences in conductance were confirmed by tracer coupling to the afferents after injection of the M-cell with Neurobiotin, where unlabeled afferents and afferents showing different degrees of staining were observed in the same dendritic area (Figure 7B). This variability of coupling was also observed for the whole population of recorded afferents. Interestingly, both the spatial distribution of CaM-KII (expressed as Periphery / Center Index; Mean = −0.11 ± 0.41 S.D., n = 43) (Figure 7D) and the coupling coefficients of individual CEs (Mean = 0.008 ± 0.003 S.D., n = 92) (Fig. 7E) showed wide variability and comparable distributions. The similarity opens the possibility that differences in the spatial distribution of CaM-KII could represent differences in the functional state of electrical synapses at these terminals, where the amount and localization of CaM-KII to gap junctions would be indicative of the degree of potentiation. Unfortunately, detecting changes in the distribution of CaM-KII following the application of the high-frequency stimulating protocols leading to synaptic potentiation (Yang et al., 1990; Pereda and Faber, 1996; Pereda et al., 1998) was impractical and difficult to interpret due to: 1) the inability of identifying the contacts in the dendrite which correspond to the sub-population of afferents stimulated by the extracellular electrode in anatomical sections and 2) to the fact that within the population of stimulated afferents, although most synapses potentiate, others were shown to depress as a result of the same stimulating protocol (see Smith and Pereda, 2003, figure 4), indicating that both depression and potentiation co-exist in the population of stimulated afferents.

DISCUSSION

> “These endings are large enough to be useful for the elucidation of many details and also for the experimental studies on which we are engaged at present.”
>
> Bartelmez and Hoerr (1933)

As pointed out by Bartelmez and Hoerr seventy-six years ago (Bartelmez and Hoerr, 1933), the unusual large size of the CEs makes them a valuable model to test specific questions regarding vertebrate synaptic transmission. The present analysis was only possible at these terminals, which offered an unparalleled access for exploring the distribution of CaM-KII within a single contact and the possibility to correlate it with well-established pharmacological and physiological properties. CEs have recently become a model for the study of interactions between chemical and electrical synapses (Pereda et al., 1998; Smith and Pereda, 2003; Pereda et al., 2004). We previously showed that within these mixed contacts the activity of glutamatergic synapses not only leads to their own potentiation but also of nearby electrical synapses (Smith and Pereda, 2003). Our results indicate that a likely major molecular candidate for this interaction is the enzyme CaM-KII. Further, our analysis of the intraterminal distribution of this kinase and its association to Cx35 indicates that CaM-KII should be considered not only a major component of glutamatergic PSDs but also of gap junction-mediated electrical synapses.

Functional significance of CaM-KII variability

A characteristic property of CaM-KII is its ability to translocate to active synaptic sites (Shen and Meyer, 1999; Merill et al., 2005; Rose et al., 2009; Gleason in al., 2003). It has been proposed that the level of CaM-KII associated with glutamatergic PSDs at any given time may be a combination of 1) transiently associated kinase, and 2) a population of this kinase that is retained after translocation and that might encode the history of correlated neuronal activity (Schulman, 2004). Translocation to contiguous synapses has been shown to occur (Rose et al., 2009; Merill et al., 2005), including to GABAergic synapses (Madsen and Caroll, personal communication), suggesting that gap junctions can also be the target of translocation/re-distribution of CaM-KII from nearby glutamatergic synapses. In contrast to glutamatergic synapses, where accumulation of this kinase at PSDs can be difficult sometimes to detect (Dosemeci et al., 2001; Merill et al., 2005), the large number and intraterminal distribution of gap junctions at CEs (predominant at the center of the contact) made it easier to detect their association with CaM-KII. Based on the association to Cx35 that we report here (see below), the distribution of CaM-KII might similarly reflect the history of synaptic activation of individual CEs. That is, the distribution of CaM-KII labeling within the population of CEs is consistent with the variability in coupling between adjacent contacts, previously shown to result from terminal-specific activity-dependent modifications initiated by glutamatergic synapses at each of these terminals (Smith and Pereda, 2003), and they both have comparable distributions. While this conclusion will require of further confirmation, there is experimental evidence that supports this possibility: 1) activated CaM-KII leads to enhancement of electrical and chemical transmission of CEs (Pereda et al., 1998), 2) the activity of CaM-KII is required for activity-dependent potentiation of CEs (Pereda et al., 1998), and finally, 3) changes in glutamatergic transmission parallel changes in electrical coupling in CEs and, accordingly, the amount of CaM-KII at individual spines of hippocampal CA1 neurons was shown to be positively correlated with the strength of its glutamatergic synapses (Asrican et. al., 2007).

Furthermore, our *in-silico* analysis and biochemical studies, in combination with our previous data (Pereda et al., 1998), suggest that association of CaM-KII with Cx35 leads to its activation, ultimately resulting in potentiation of electrical transmission in CEs. According to current models (Bayer et al., 2001; Schulman, 2004) the binding of CaM-KII to Cx36 (Alev et al., 2008) and likely to Cx35 (based on the sequence homology and Co-IP we report here), will lock this kinase in a persistently active state, even after dissociation of calmodulin. More specifically, the αCaM-KII autoinhibitory domain is considered a gate consisting of a pseudosubstrate segment, that blocks binding of substrates to the “S site”, as well as a pseudotarget segment that blocks access to its target proteins (“T site”) (Bayer et al., 2001; Hudmon and Schulman, 2002; Schulman, 2004). Binding of Ca^{++}/calmodulin opens the gate and allows substrates to bind (kinase activation), thereby enabling interactions with some targets such as to the NR2B subunit of the NMDA receptor (Bayer et al., 2001), Drosophila Eag potassium channel (Sun et al., 2004) and Cx36 (Alev et al., 2008) all of which contain similar “pseudosubstrate” and “pseudotarget” binding regions. This mechanism would be equivalent to the classic effect of autophosphorylation of Thr286, positioned like a “wedge” in the inhibitory gate, further displacing it (Singla et al., 2001; Schulman, 2004) and enabling interactions with additional targeting proteins (Bayer et al., 2001; Schulman, 2004). As mentioned above, our previous work showed that intradendritic injections of a constitutively active form of αCaM-KII in the M-cell led to a persistent potentiation of the electrical component of the mixed synaptic potential evoked by stimulation of CEs and CaM-KII activation was found to be required for the induction of activity-dependent potentiation of this synaptic potential (Pereda et al. 1998). Taken together, these evidence suggest that the activity of CaM-KII indeed leads to potentiation of electrical transmission in CEs, and differences in the spatial distribution of this kinase could thus represent differences in the functional state of

electrical synapses at these terminals, where the amount and localization of CaM-KII to gap junctions would be indicative of the degree of potentiation.

Our current experimental approaches made impractical to detect changes in the distribution of CaM-KII following activity-dependent protocols. This question could be more easily addressed in future experiments using zebrafish embryos, where it is possible to track the translocation and/or redistribution of fluorescently-tagged kinase to synaptic sites (Gleason, 2003). Nonetheless, these results provide, for the first time, evidence of the distribution and association of CaM-KII to identifiable electrical synapses *in-vivo*, where it is possible to correlate the presence of this kinase with its known functional properties.

CaM-KII regulatory mechanisms are conserved

The *in-silico* analysis revealed the existence of multiple phosphorylation sites for αCaM-KII in Cx35. These predictions were consistent with those recently reported for Cx36, (Alev et al., 2008), which were confirmed by biochemical approaches, providing a high degree of confidence on this analysis. By extending our analysis to an additional fish homolog of Cx36, Cx34.7, we found that Cx36, Cx35, and Cx34.7 shared most of the identified residues. The analysis also showed that residues S315 / S298 / S300 in Cx36, Cx35 and Cx34.7, respectively, constitute exclusive phosphorylation sites for CaM-KII that are not shared with other kinases. On the other hand, residues S110 and S293 in Cx36, S110 and S276 in Cx35, and S110 and S277 in Cx34.7, are phosphorylation sites shared with cAMP-dependent protein kinase A (O'Brien et al., 1998; Mitropoulou and Bruzzone, 2003; Ouyang et al., 2005; Urschel et al., 2006), a kinase also shown to promote enhancement of electrical transmission at these terminals (Pereda et al., 1994; Cachope et al., 2007). Interestingly, our IP experiments (restricted to a small portion of the hindbrain that mainly contains the M-cells) showed multiple bands for Cx35 pulled down by CaM-KII. Although final proof would require dephosphorylation of samples with protein phosphatase, this observation is consistent with the possibility that Cx35 coexists at multiple states of phosphorylation. We did not investigate this possibility further, which will be the focus of future research efforts. In summary, our sequence alignment shows that CaM-KII binding regions and phosphorylation sites are highly similar between Cx36 and its fish homologs, indicating that essential regulatory mechanisms are highly conserved and likely to pertain to all Cx35- and Cx36-mediated electrical synapses. These mechanisms could include, as shown for glutamate receptors, direct phosphorylation of the channels themselves (Derkach et al., 1999) or the promotion of their insertion in the plasma membrane (Shi et al., 1999; Liao at al., 2001; Shi et al., 2001).

CaM-KII is a non-obligatory component of electrical synapses

In contrast to the extensive information on proteins associated with chemical synapses (Kim and Sheng, 2004) involved in channel insertion, anchoring or removal from the plasma membrane (Lin et al., 2004; Malinow et al., 2000; Migaud et al., 1998; Mori et al., 1998; Shi et al., 1999; Sprengel et al., 1998; Steigerwald et al., 2000), very few proteins have been shown to associate to the neuronal gap junctions. It is currently accepted that gap junctions are not only comprised of the defining intercellular channel proteins, but also associated scaffold and regulatory proteins (Herve et al., 2004). Neuronal gap junctions in particular, characteristically exhibit a PSD-like structure in EM, described as a "semi-dense cytoplasmatic matrix" (Sotelo and Korn, 1978), and which likely represents (similar to glutamatergic PSDs) proteins associated with these intercellular channels. Cx36 (Condorelli et al., 1998), the most prevalent neuronal connexin that is widely distributed throughout the mammalian brain (Condorelli et al., 2000), was shown to interact with two relevant proteins: CaM-KII (Alev et al., 2008) and ZO-1 (Li et al., 2004). ZO-1 is a member of the MAGUK family of proteins which was reported to interact with several other connexins (Itoh et al., 1999). Our recent work indicates that ZO-1 also interacts with Cx35 in CEs (Flores et al., 2008). Because its co-localization with Cx35 is

extensive (Flores et al., 2008), ZO-1 is likely to play a structural role and the properties of the ZO-1/Cx35 association suggest the existence of a dynamic relation between these two proteins, possibly including a role of ZO-1 in regulating gap junctional conductance at these highly modifiable electrical synapses (Flores et al., 2008). Our present results show that CaM-KII also associates with Cx35 at CEs. This study extends the observations of Alev and colleagues (Alev et al., 2008) showing that CaM-KII associates with neuronal connexins in anatomically identifiable, native, electrical synapses. More importantly, our data also indicates that CaM-KII is likely a non-obligatory component of electrical synapses. That is, its presence is highly variable, even between gap junction plaques within the same contact, and likely is linked to differences in the degree of potentiation between individual terminals (see above). In comparison with ZO-1, which would play a more permanent or structural role, the presence of CaM-KII seems to be non-obligatory and possibly regulated by neural activity (Fig. 8). This conclusion is consistent with the dynamic translocation properties of CaM-KII and whose presence is thought to represent the history of synaptic activation. Thus, our results indicate that ZO-1 and CaM-KII probably belong to the same macromolecular complex, and together with other identified proteins [association to zonula occludens proteins ZO-2 (Ciolofan et al., 2006) and ZO-3 (Li et al., 2009) and calmodulin (Burr et al., 2005) were also reported] as well as those that might be identified in the future, are likely components of the “semi-dense cytoplasmatic matrix”, associated with intercellular channels in neuronal gap junctions.

In summary, CaM-KII is not only a major component of glutamatergic postsynaptic densities but is also an important and dynamic component of gap junction-mediated electrical synapses in CEs. Given the widespread distribution of Cx35- and Cx36-mediated electrical synapses, our data suggest that the properties observed at these identifiable gap junctions might also apply to electrical synapses elsewhere, including those in mammalian brain.

Supplementary Material

Refer to Web version on PubMed Central for supplementary material.

Acknowledgments

This research was supported by National Institutes of Health grants DC03186 and NS0552827 (to A.E. Pereda). We thank Carl Castillo for help with immunochemistry and Joseph Zavilovitz for help with the confocal microscope during initial experiments. We also thank Costa Dobrenis and the Morphology Core of the Rose F. Kennedy Center for outstanding support. Finally, we thank David Spray, Rolf Dermietzel and Theresa Szabo for useful discussions and comments on the manuscript.

References

Alev C, Urschel S, Sonntag S, Zoidl G, Fort AG, Höher T, Matsubara M, Willecke K, Spray DC, Dermietzel R. The neuronal connexin36 interacts with and is phosphorylated by CaMKII in a way similar to CaMKII interaction with glutamate receptors. Proc Natl Acad Sci U S A 2008;105:20964–20969. [PubMed: 19095792]

Asrican B, Lisman J, Otmakhov N. Synaptic strength of individual spines correlates with bound Ca2+-calmodulin-dependent kinase II. J Neurosci 2007;27:14007–14011. [PubMed: 18094239]

Bayer KU, De Koninck P, Leonard AS, Hell JW, Schulman H. Interaction with the NMDA receptor locks CaMKII in an active conformation. Nature 2001;411:801–805. [PubMed: 11459059]

Bartelmez GW. Mauthner's cell and the nucleus motorius tegmenti. J Comp Neurol 1915;25:87–128.

Bartelmez GW, Hoerr NL. The vestibular club endings in Ameiurus. Further evidence on the morphology of the synapse. J Comp Neurol 1933;67:401–428.

Bodian D. The structure of the vertebrate synapse. A study of the axon endings on Mauthner’s cell and neighboring centers in the goldfish. J Comp Neurol 1937;1:117–160.

Burr GS, Mitchell CK, Keflemariam YJ, Heidelberger R, O'Brien J. Calcium-dependent binding of calmodulin to neuronal gap junction proteins. Biochem Biophys Res Commun 2005;335:1191–1198. [PubMed: 16112650]

Cachope R, Mackie K, Triller A, O'Brien J, Pereda AE. Potentiation of electrical and chemical synaptic transmission mediated by endocannabinoids. Neuron 2007;56:1034–1047. [PubMed: 18093525]

Ciolofan C, Li XB, Olson C, Kamasawa N, Gebhardt BR, Yasumura T, Morita M, Rash JE, Nagy JI. Association of connexin36 and zonula occludens-1 with zonula occludens-2 and the transcription factor zonula occludens-1-associated nucleic acid-binding protein at neuronal gap junctions in rodent retina. Neuroscience 2006;140:433–451. [PubMed: 16650609]

Condorelli DF, Parenti R, Spinella F, Trovato Salinaro A, Belluardo N, Cardile V, Cicirata F. Cloning of a new gap junction gene (Cx36) highly expressed in mammalian brain neurons. Eur J Neurosci 10:1202–1208. [PubMed: 9753189]

Condorelli DF, Belluardo N, Trovato-Salinaro A, Mudo G. Expression of Cx36 in mammalian neurons. Brain Res Rev 2000;32:72–85. [PubMed: 10751658]

Connors BW, Long MA. Electrical synapses in the mammalian brain. Annu Rev Neurosci 2004;27:393–418. [PubMed: 15217338]

Curti S, Pereda A. Voltage-dependent enhancement of electrical coupling by a sub-threshold sodium current. J Neurosc 2004;24:3999–4010.

Curti S, Gomez L, Budelli R, Pereda A. Subthreshold sodium current underlies essential functional specializations at primary auditory afferents. Journal of Neurophysiology 2008;99:1683–1699. [PubMed: 18234982]

Derkach V, Barria A, Soderling TR. Ca2+/calmodulin-kinase II enhances channel conductance of α-amino-3-hydroxy-5-methyl-isoxazolepropionate type glutamate receptors. Proc Natl Acad Sci USA 1999;96:3269–3274. [PubMed: 10077673]

Dosemeci A, Tao-Cheng JH, Vinade L, Winters CA, Pozzo-Miller L, Reese TS. Glutamate-induced transient modification of the postsynaptic density. Proc Natl Acad Sci U S A 2001;98:10428–10432. [PubMed: 11517322]

Fink CC, Meyer T. Molecular mechanisms of CaMKII activation in neuronal plasticity. Curr Opin Neurobiol 2002;12:293–299. [PubMed: 12049936]

Flores C, Li X, Bennett MVL, Nagy JI, Pereda A. Interaction between connexin 35 and zonula occludens 1 and its potential role in regulation of electrical synapses, Proc. Natl Acad Sci (USA) 2008;105:12545–12550.

Fukami Y, Furukawa T, Asada Y. Excitability changes of the Mauthner cell during collateral inhibition. J Gen Physiol 1965;48:581–600. [PubMed: 14324977]

Furshpan EJ. “Electrical transmission” at an excitatory synapse in a vertebrate brain. Science 1964;144:878–880. [PubMed: 14149407]

Gleason MR, Higashijima S, Dallman J, Liu K, Mandel G, Fetcho JR. Translocation of CaM kinase II to synaptic sites in vivo. Nat Neurosci 2003;6:217–218. [PubMed: 12563265]

Herve JC, Bourmeyster N, Sarrouilhe D. Diversity in protein-protein interactions of connexins: emerging roles. Biochim Biophys Acta 2004;1662:22–41. [PubMed: 15033577]

Itoh M, Furuse M, Morita K, Kubota K, Saitou M, Tsukita S. Direct binding of three tight junction-associated MAGUKs, ZO-1, ZO-2, and ZO-3, with the COOH termini of claudins. J Cell Biol 1999;147:1351–1363. [PubMed: 10601346]

Kim E, Sheng M. PDZ domain proteins of synapses. Nat Rev Neurosci 2004;5:771–781. [PubMed: 15378037]

Kothmann WW, Li X, Burr GS, O'Brien J. Connexin 35/36 is phosphorylated at regulatory sites in the retina. Vis Neurosci 2007;24:363–375. [PubMed: 17640446]

Lee SJ, Escobedo-Lozoya Y, Szatmari EM, Yasuda R. Activation of CaMKII in single dendritic spines during long-term potentiation. Nature 2009;458:299–304. [PubMed: 19295602]

Liao D, Scannevin RH, Huganir R. Activation of silent synapses by rapid activity-dependent synaptic recruitment of AMPA receptors. J Neurosci 2001;21:6008–6017. [PubMed: 11487624]

Li X, Olson C, Lu S, Kamasawa N, Yasumura T, Rash JE, Nagy JI. Neuronal connexin36 association with zonula occludens-1 protein (ZO-1) in mouse brain and interaction with the first PDZ domain of ZO-1. Eur J Neurosci 2004;19:2132–2146. [PubMed: 15090040]

Li X, Olson C, Lu S, Nagy JI. Association of connexin36 with zonula occludens-1 in HeLa cells, betaTC-3 cells, pancreas, and adrenal gland. Histochem Cell Biol 2004;122:485–498. [PubMed: 15558297]

Li X, Lu S, Nagy JI. Direct association of connexin36 with zonula occludens-2 and zonula occludens-3. Neurochem Int 2009;54:393–402. [PubMed: 19418635]

Lin JW, Faber DS. Synaptic transmission mediated by single club endings on the goldfish Mauthner cell. I Characteristics of electrotonic and chemical postsynaptic potentials. J Neurosci 1988a;8:1302–1312. [PubMed: 2833580]

Lin JW, Faber DS. Synaptic transmission mediated by single club endings on the goldfish Mauthner cell. II Plasticity of excitatory postsynaptic potentials. J Neurosci 1998b;8:1313–25. [PubMed: 2833581]

Lin Y, Skeberdis VA, Francesconi A, Bennett MVL, Zukin RS. Postsynaptic density protein-95 regulates NMDA channel gating and surface expression. J Neurosci 2004;24:10138–10148. [PubMed: 15537884]

Malinow R, Mainen ZF, Hayashi Y. LTP mechanisms: from silence to four-lane traffic. Curr Opin Neurobiol 2000;10:352–357. [PubMed: 10851179]

Merrill MA, Chen Y, Strack S, Hell JW. Activity-driven postsynaptic translocation of CaMKII. Trends Pharmacol Sci 2005;26:645–53. [PubMed: 16253351]

Migaud M, Charlesworth P, Dempster M, Webster LC, Watabe AM, Makhinson M, He Y, Ramsay MF, Morris RG, Morrison JH, O'Dell TJ, Grant SG. Enhanced long-term potentiation and impaired learning in mice with mutant postsynaptic density-95 protein. Nature 1998;396:433–439. [PubMed: 9853749]

Mitropoulou G, Bruzzone R. Modulation of perch connexin35 hemi-channels by cyclic AMP requires a protein kinase A phosphorylation site. J Neurosci Res 2003;72:147–57. [PubMed: 12671989]

Mori H, Manabe T, Watanabe M, Satoh Y, Suzuki N, Toki S, Nakamura K, Yagi T, Kushiya E, Takahashi T, Inoue Y, Sakimura K, Mishina M. Role of the carboxy-terminal region of the GluR epsilon2 subunit in synaptic localization of the NMDA receptor channel. Neuron 1998;21:571–580. [PubMed: 9768843]

Ohta Y, Nishida E, Sakai H. Type II Ca2+/calmodulin-dependent protein kinase binds to actin filaments in a calmodulin-sensitive manner. FEBS Lett 1986;208:423–426. [PubMed: 3780978]

O'Brien J, Bruzzone R, White TW, Al-Ubaidi MR, Ripps H. Cloning and expression of two related connexins from the perch retina define a distinct subgroup of the connexin family. J Neurosci 1998;18:7625–7637. [PubMed: 9742134]

Ouyang X, Winbow VM, Patel LS, Burr GS, Mitchell CK, O'Brien J. Protein kinase A mediates regulation of gap junctions containing connexin35 through a complex pathway. Brain Res Mol Brain Res 2005;135:1–11. [PubMed: 15857663]

Pereda A, Nairn A, Wolszon L, Faber DS. Postsynaptic modulation of synaptic efficacy at mixed synapses on the Mauthner cell. J Neurosci 1994;14:3704–3712. [PubMed: 8207483]

Pereda AE, Faber DS. Activity dependent short-term plasticity of intercellular coupling. J Neurosci 1996;16:983–992. [PubMed: 8558267]

Pereda A, Bell T, Chang B, Czernik A, Nairn A, Soderling T, Faber DS. Ca^{2+}/calmodulin-dependent kinase II mediates simultaneous enhancement of gap junctional conductance and glutamatergic transmission. Proc Natl Acad Sci USA 1998;95:3272–13277.

Pereda A, O'Brien J, Nagy JI, Bukauskas F, Davidson KG, Kamasawa N, Yasumura T, Rash JE. Connexin35 mediates electrical transmission at mixed synapses on Mauthner cells. J Neurosci 2003;23:7489–503. [PubMed: 12930787]

Pereda AE, Rash JE, Nagy JI, Bennett MVL. Dynamics of electrical transmission at club endings on the Mauthner cells. Brain Res Rev 2004;47:227–244. [PubMed: 15572174]

Robertson J, Bodenheimer TS, Stage DE. The ultrastructure of Mauthner cell synapses and nodes in goldfish brains. J Cell Biol 1963;19:159–199. [PubMed: 14069792]

Rose J, Jin SX, Craig AM. Heterosynaptic molecular dynamics: locally induced propagating synaptic accumulation of CaM kinase II. Neuron 2009;61:351–358. [PubMed: 19217373]

Rosenberg OS, Deindl S, Sung RJ, Nairn AC, Kuriyan J. Structure of the autoinhibited kinase domain of CaMKII and SAXS analysis of the holoenzyme. Cell 2005;123:849–8460. [PubMed: 16325579]

Sahyoun N, LeVine H, Bronson D, Siegel-Greenstein F, Cuatrecasas P. Cytoskeletal calmodulin-dependent protein kinase. Characterization, solubilization, and purification from rat brain. J Biol Chem 1985;260:1230–1237. [PubMed: 4038501]

Steigerwald F, Schulz TW, Schenker LT, Kennedy MB, Seeburg PH, Köhr G. C-Terminal truncation of NR2A subunits impairs synaptic but not extrasynaptic localization of NMDA receptors. J Neurosci 2000;20:4573–4581. [PubMed: 10844027]

Shen K, Meyer T. Dynamic control of CaMKII translocation and localization in hippocampal neurons by NMDA receptor stimulation. Science 1999;28:162–166. [PubMed: 10102820]

Shi SH, Hayashi Y, Petralia RS, Zaman SH, Wenthold RJ, Svoboda K, Malinow R. Rapid spine delivery and redistribution of AMPA receptors after synaptic NMDA receptor activation. Science 1999;284:1811–1816. [PubMed: 10364548]

Shi S, Hayashi Y, Esteban JA, Malinow R. Subunit-specific rules governing AMPA receptor trafficking to synapses in hippocampal pyramidal neurons. Cell 2001;105:331–343. [PubMed: 11348590]

Schulman H. Activity-dependent regulation of calcium/calmodulin-dependent protein kinase II localization. J Neurosci 2004;24:8399–8403. [PubMed: 15456811]

Smith M, Pereda AE. Chemical synaptic activity modulates nearby electrical synapses. Proc Natl Acad Sci USA 2003;100:4849–4854. [PubMed: 12668761]

Sotelo C, Korn H. Morphological correlates of electrical and other interactions through low-resistance pathways between neurons of the vertebrate central nervous system. Internat Rev Cytol 1978;55:67–107.

Sprengel R, Suchanek B, Amico C, Brusa R, Burnashev N, Rozov A, Hvalby O, Jensen V, Paulsen O, Andersen P, Kim JJ, Thompson RF, Sun W, Webster LC, Grant SG, Eilers J, Konnerth A, Li J, McNamara JO, Seeburg PH. Importance of the intracellular domain of NR2 subunits for NMDA receptor function in vivo. Cell 1998;92:279–289. [PubMed: 9458051]

Strack S, McNeill RB, Colbran RJ. Mechanism and regulation of calcium/calmodulin-dependent protein kinase II targeting to the NR2B subunit of the N-methyl-D-aspartate receptor. J Biol Chem 2000;275:23798–23806. [PubMed: 10764765]

Sun XX, Hodge JJ, Zhou Y, Nguyen M, Griffith LC. The eag potassium channel binds and locally activates calcium/calmodulin-dependent protein kinase II. J Biol Chem 2004;279:10206–10214. [PubMed: 14699099]

Tuttle R, Masuko S, Nakajima Y. Freeze fracture study of the Large Myelinated Club Ending synapse on the goldfish Mauthner cell: special reference to the quantitative analysis of gap junctions. J Comp Neurol 1986;246:202–211. [PubMed: 3007585]

Urschel S, Höher T, Schubert T, Alev C, Söhl G, Wörsdörfer P, Asahara T, Dermietzel R, Weiler R, Willecke K. Protein kinase A-mediated phosphorylation of connexin36 in mouse retina results in decreased gap junctional communication between AII amacrine cells. J Biol Chem 2006;281:33163–33171. [PubMed: 16956882]

Wayman GA, Lee YS, Tokumitsu H, Silva A, Soderling TR. Calmodulin-kinases: modulators of neuronal development and plasticity. Neuron 2008;59:914–931. [PubMed: 18817731]

Wolszon L, Pereda AE, Faber DS. A fast synaptic potential mediated by NMDA and non-NMDA receptors. J Neurophysiol 1997;78:2693–2706. [PubMed: 9356419]

Xue Y, Ren J, Gao X, Jin C, Wen L, Yao X. GPS 2.0, a Tool to Predict Kinase-specific Phosphorylation Sites in Hierarchy. Mol Cell Proteomics 2008;7:1598–1608. [PubMed: 18463090]

Yang E, Schulman H. Structural examination of autoregulation of multifunctional calcium/calmodulin-dependent protein kinase II. J Biol Chem 1999;274:26199–26208. [PubMed: 10473573]

Yang XD, Korn H, Faber DS. Long-term potentiation of electrotonic coupling at mixed synapses. Nature 1990;348:542–545. [PubMed: 2174130]

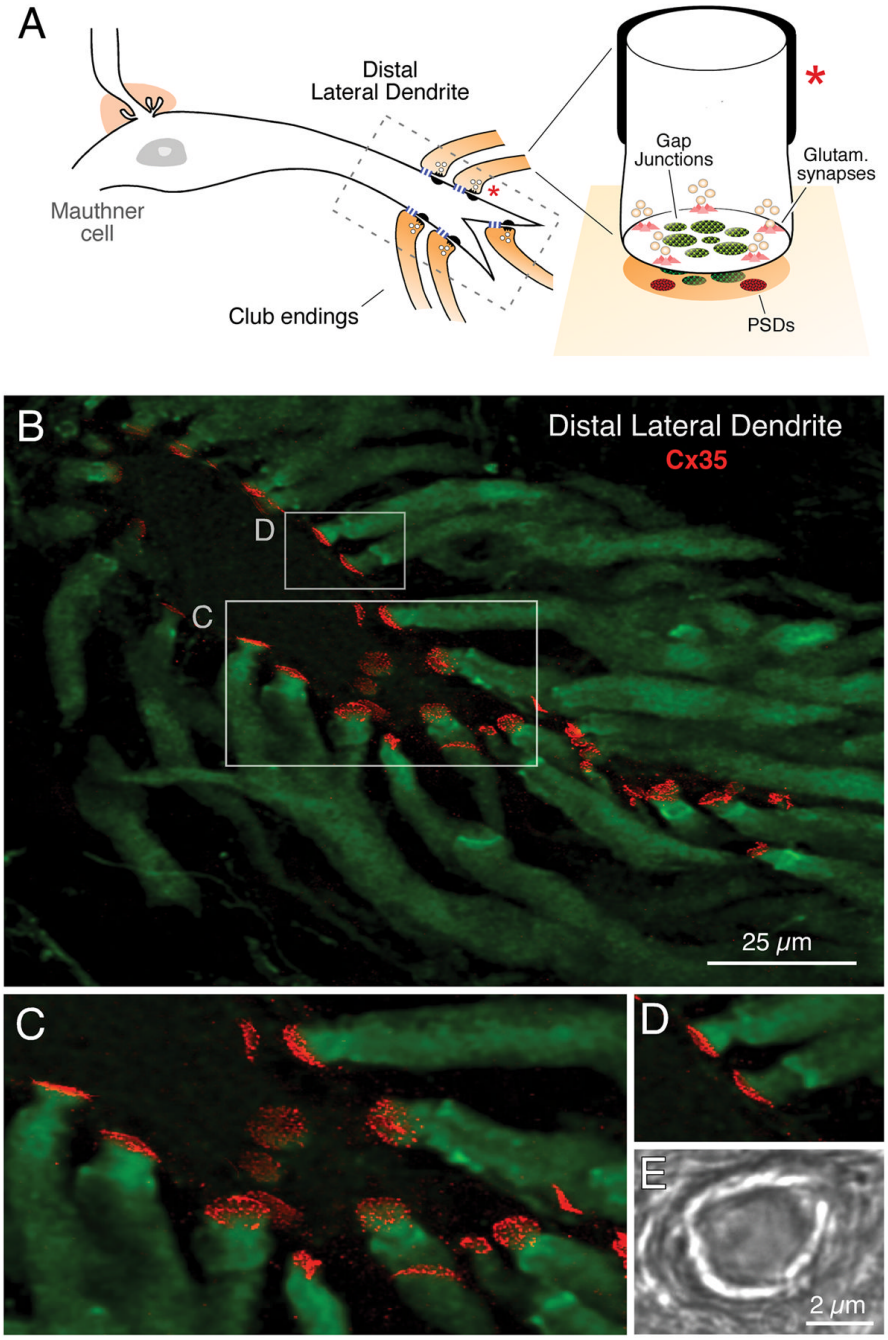

Figure 1. The Club endings: the striking synapses of the Mauthner cell

(A) Diagram of the M-cell showing its axon cap, soma and lateral dendrite. The Large Myelinated Club endings, referred to here as "Club endings" (CEs), are distributed along the distal portion of the lateral dendrite. These contacts belong to primary auditory afferents that establish mixed (electrical and chemical) synapses on the distal portion of the M-cell lateral dendrite. Right: The cartoon summarizes the main structural features of CEs; specializations corresponding to chemical synapses are restricted to the periphery of the contact. The pre and post-synaptic elements of the synapse are illustrated separately, for better appreciation of the PSDs. (B) Projection image of the distal portion of the lateral dendrite obtained with laser scanning confocal microscopy, illustrating saccular afferents (green) terminating as CEs.

Labeling of these afferents was obtained using a phospho-specific anti-Cx35 antibody (Cx35 phospho-Ser110), which is known to cross react to unknown high molecular weight phosphoproteins that appear to be expressed primarily in glial cells (Kothmann et al. 2007). Double-labeling with monoclonal anti-Cx35/36 antibody (red; Chemicon) reveals the area of contact between CEs and the distal portion of the M-cell lateral dendrite. (C) Higher magnification of the labeled boxed region in B. The observation of multiple Cx35-labeled puncta is consistent with the presence of up to ~200 gap junction plaques in individual CEs. (D) Higher magnification of the labeled boxed region in B. Cx35 labeling is observed at the region of contact between two CEs and the M-cell dendrite. (E) Image of a Club ending on the surface of the lateral dendrite obtained using DIC optics. These unusually large contacts are easily recognizable due to their big size and characteristic ring-like appearance due to their prominent myelinization.

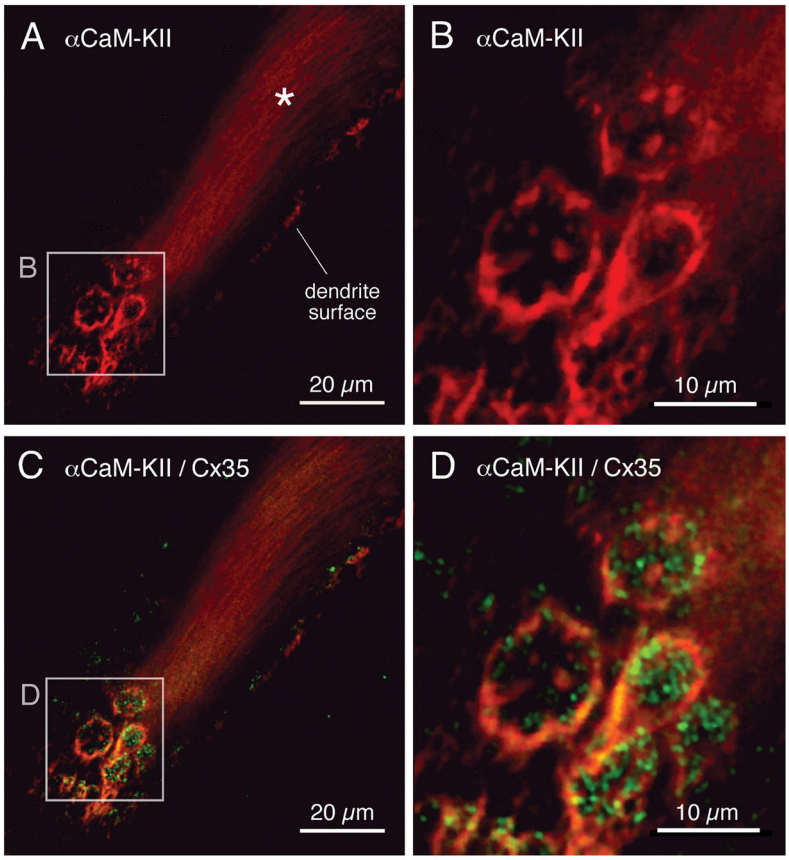

Figure 2. Double-immunolabeling of Cx35 and αCaM-KII in the lateral dendrite of the Mauthner cells

(A) Laser scanning confocal projection image of the distal portion of the M-cell lateral dendrite (average of 5 sections) using a polyclonal anti-αCaM-KII antibody (G-301; red). The G-301 antibody also labeled neurofilaments (asterisks) in the cytoskeleton of the M-cell. (B) Higher magnification of the labeled boxed region in A, illustrating αCaM-KII labeling at individual CEs. (C) Double-labeling using the polyclonal anti-αCaM-KII (G-301; red) and anti-Cx35/36 (green) antibodies respectively. (D) High magnification of the labeled boxed region in C.

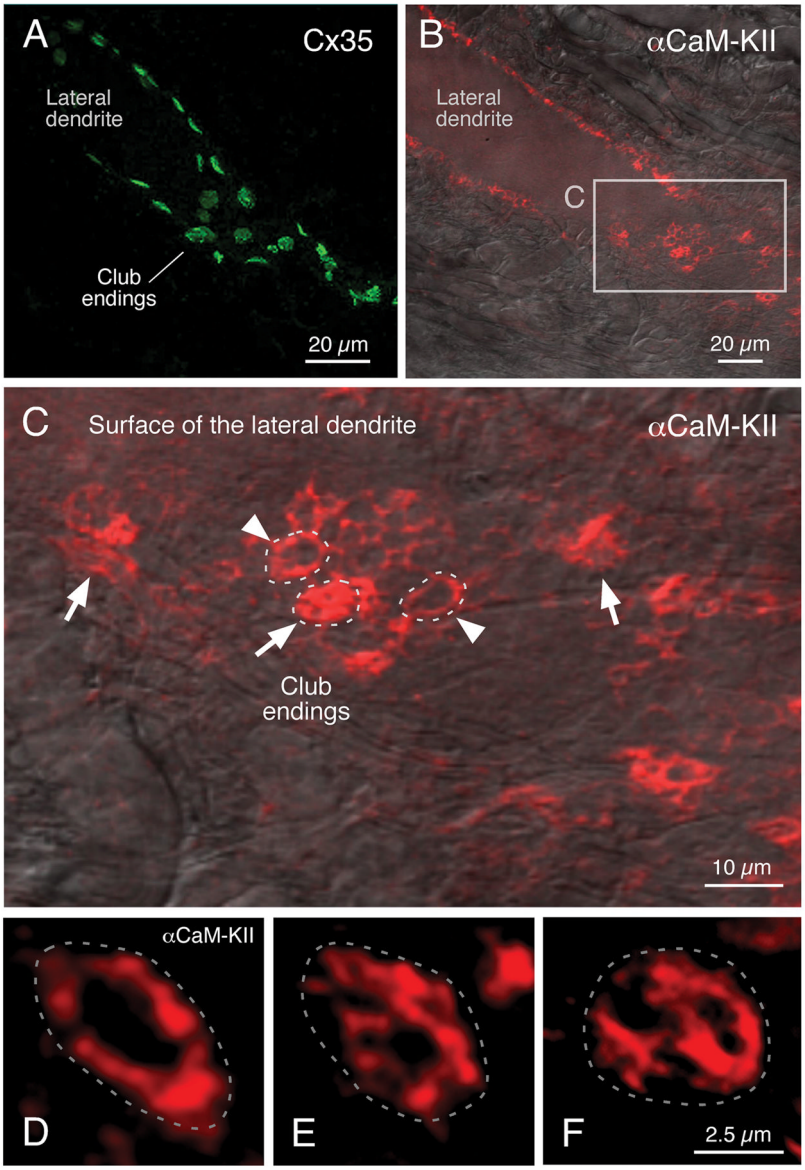

Figure 3. Heterogeneity of αCaM-KII labeling between contiguous Club endings

(A) Confocal projection of the distal portion of the lateral dendrite showing Immunolabeling for Cx35 using monoclonal anti-Cx35/36 antibody. Note the regularity of Cx35 labeling between CEs. (B) Confocal projection of a similar portion of the distal lateral dendrite showing immunolabeling for αCaM-KII (G301 antibody). (C) Higher magnification of the labeled boxed region in B. CaM-KII distribution is highly variable between adjacent CEs (arrowheads: predominant in the terminal periphery; arrows: predominant on the entire surface of the contact).

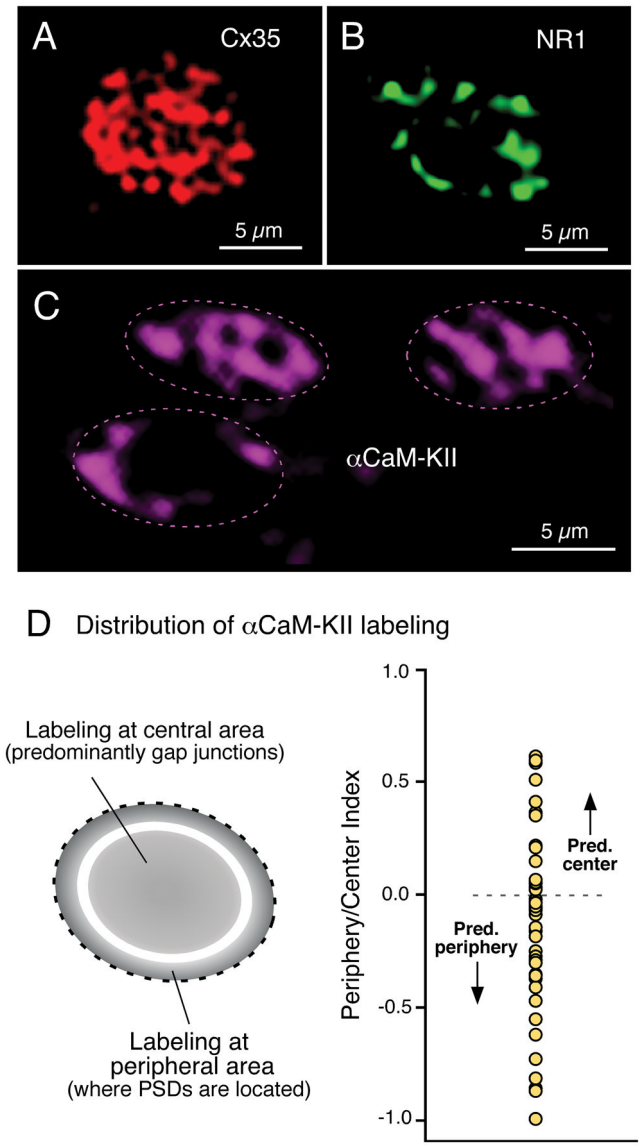

Figure 4. Intraterminal distribution of αCaM-KII in Club endings

Confocal projections of individual Club endings showing the distribution of Cx35 (A), NR1 (B) and αCaM-KII (C). (A–B) Cx35 labeling is typically punctate and covers most of the surface contact area whereas NR1 labeling is mostly restricted to the periphery of the synaptic contact (images in panels A and B were previously illustrated; Pereda et al., 2003). (C) In contrast, αCaM-KII labeling (G-301 antibody) is more diffuse and highly variable between contiguous Club endings. While αCaM-KII labeling was always observed at the periphery, where PSDs are located, it is also found at the center of the CEs contact area in some cases (compare top CEs with the bottom one). (D) Quantification of the variability of αCaM-KII distribution of CEs using a ratio between the labeling at periphery and center of each CE. Diagram of the regions selected for analysis: a peripheral "ring" area (where PSDs are included) and a center area (where gap junctions are predominant). A transition area (white) between periphery and center areas was not included in the analysis. The ratio between these areas was defined as "Periphery-Center Index" (see Methods for detail). Graph illustrates the distribution of this index for 43 Club endings.

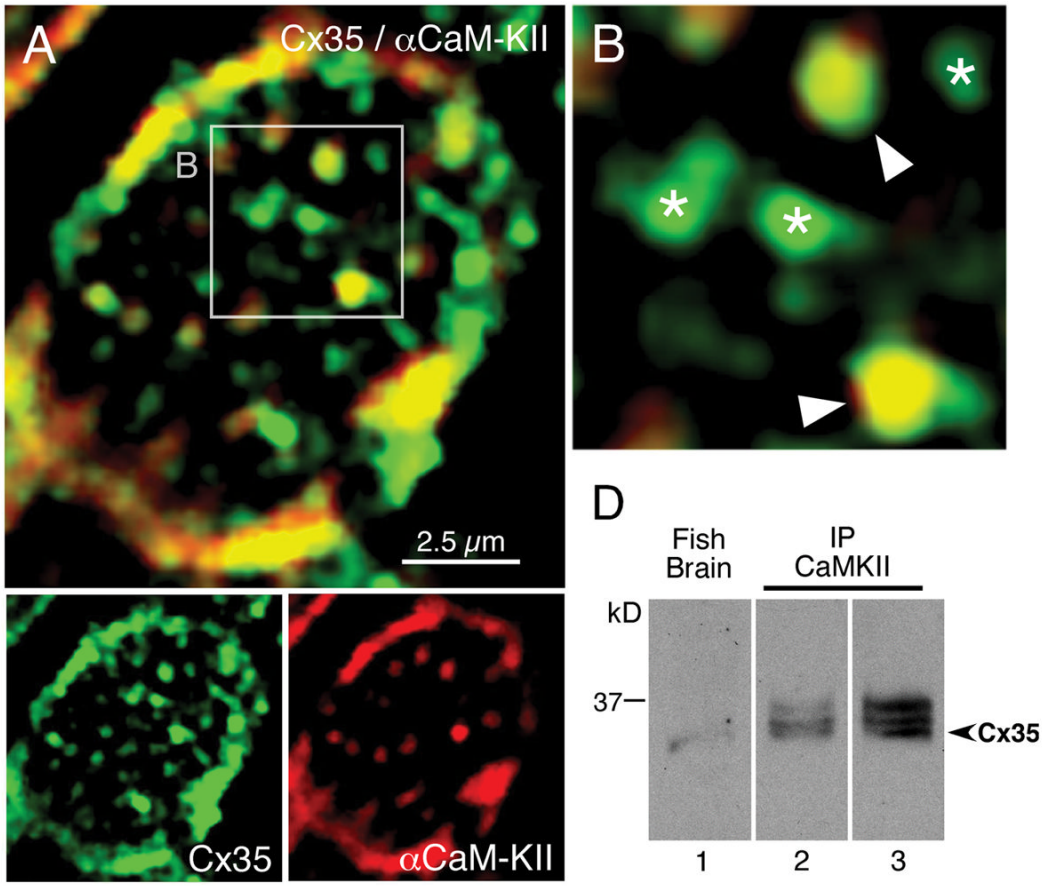

C Regions containing binding sites to αCaM-KII

Cytoplasmic loop binding site — 86%

```
            181                  201
mCx36        LRTAARSKLRRQEGISRFYII
             :|| .:||:||||||||||||
pCx35       AMRT-TKSKMRRQEGISRFYII
            164                  184
```

Carboxyl-terminal binding site — 92%

```
            275                  299
             LGWRKIKLAVRGAQAKRKSVYEIRN
             |||||||.||||.||:|||:|||||
            LGWRKIKTAVRGVQARRKSIYEIRN
            258                  282
```

Figure 5. Connexin35 and αCaM-KII co-localize at Club endings and associate in goldfish brain

(A) Confocal z-section of a single terminal showing co-localization (yellow) of Cx35 (green) and αCaM-KII (red). Labeling of Cx35 and αCaM-KII co-localizes at the periphery and the center of the synaptic contact. (B) Higher magnification of the labeled boxed region in B. αCaM-KII and Cx35 co-localize at some Cx35 puncta (arrowheads), but is absent at others (asterisks). (C) Sequence alignment of mCx36 cytoplasmic loop and carboxyl-terminal αCaM-KII binding site regions (Alev et al, 2008) reveals a high-degree of similarity with pCx35 (86% and 92%, respectively). (D) Immunoblot detection of Cx35 in two different samples (lanes 2 and 3) with mCx35/36 antibody after immunoprecipitation (IP) of αCaM-KII from goldfish hindbrain with G301 antibody. The Cx35 immunoblot exhibits three identifiable bands.

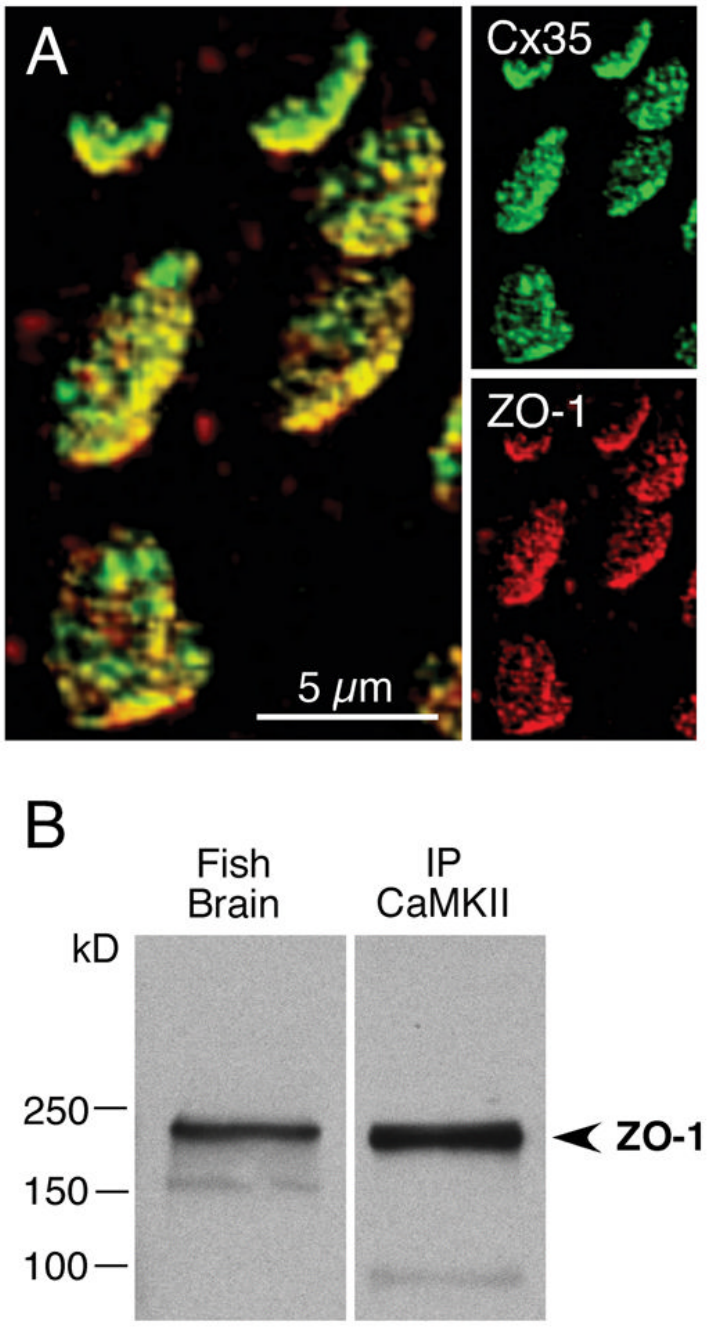

Figure 6. αCaM-KII associates with Zonula occludens-1 (ZO-1) in goldfish brain

(A) Extensive co-localization of Cx35 (green) and ZO-1 (red) at CEs in the M-cell lateral dendrite. (B) Immunoblot detection of ZO-1 (lane 2) with mZO-1 antibody after IP of αCaM-KII from goldfish hindbrain with G301 antibody.

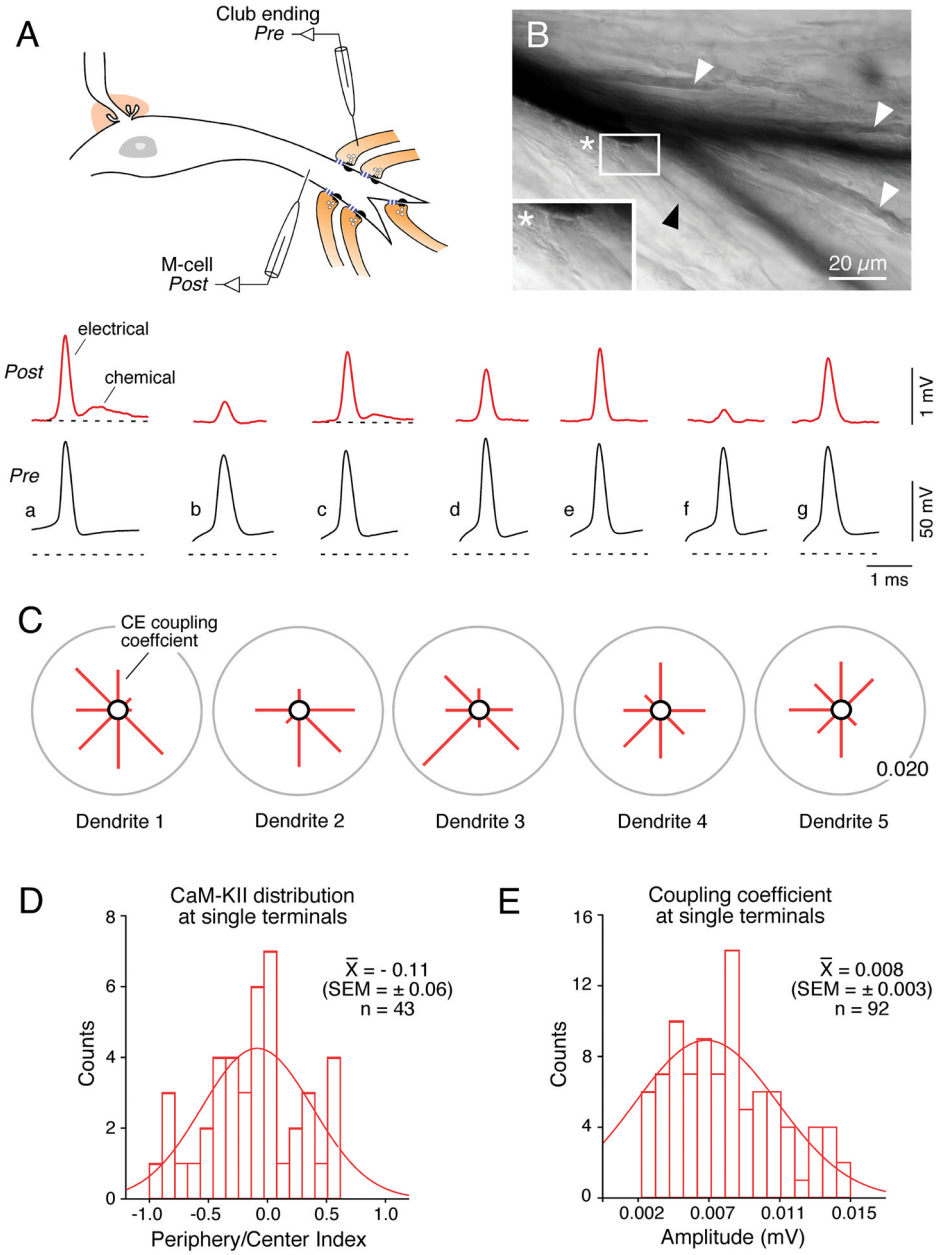

Figure 7. Electrical synapses between neighboring Club endings co-exist at different degrees of conductance on the M-cell lateral dendrite

(A) Differences in gap junctional conductance between CEs evidenced by multiple simultaneous recordings in the same M-cell dendrite. The recordings of unitary synaptic potentials (red top traces) were obtained sequentially from the same dendritic position and it cannot be explained by differences in the amplitude of the presynaptic action potentials (black lower traces), where variability was much lower. Only two of these nine unitary synaptic potentials exhibit a clear chemical component (e.g.: “chemical” in recording “a”). (B) Variability in the amplitude of unitary coupling potentials does not represent variability in the electrotonic distances from the recording site, as a similar diversity in coupling strength can be revealed using neurobiotin dye coupling (see also Smith and Pereda, 2003). Transfer of neurobiotin from the M-cell to neighboring CEs differs dramatically (dark, white arrowheads,

and unlabeled, black arrowheads), indicating that junctions differ in permeability. View of the bifurcation of the lateral dendrite (dark branches) obtained with DIC optics and revealing differences of labeling between neighboring CEs (only a small number of CEs are generally labeled following injection of neurobiotin into the M-cell indicating that gap junction permeability at CEs is generally low). Inset: A single terminal distinguished solely by the use of DIC optics. (C) Variability of coupling coefficients amongst individual CEs in five different fish. Inner circle represents the M-cell lateral dendrite. The length of each line is proportional to the coupling coefficient of that CE. For calibration, the circle represents a coupling potential of 0.020. (D) Histogram showing the periphery/center index distribution of the CaM-KII distribution at single terminals (n=43). (E) Histogram showing the amplitude distribution of the unitary electrical EPSPs (n = 92).

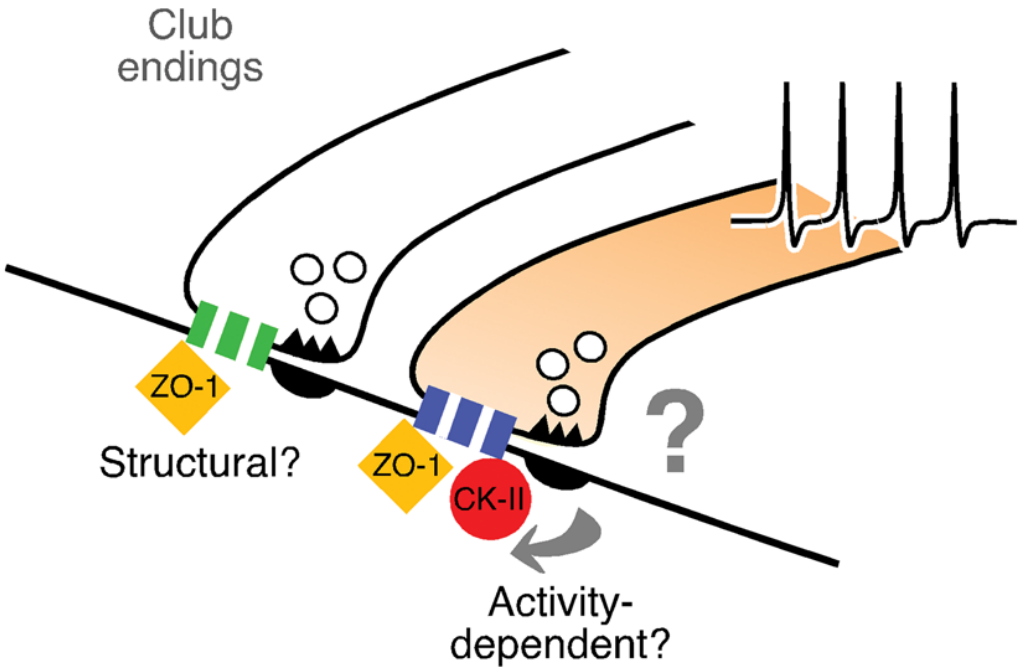

Figure 8. Potential mechanism for differences in CaM-KII labeling between contiguous Club endings

Electrical synapses at adjacent CEs co-exist at different degrees of conductance (indicated by different colors). The extensive co-localization of Cx35 with ZO-1 suggests that this scaffold protein could constitute a structural component of gap junctions at these terminals. Activity of neighboring chemically transmitting regions within the terminal trigger changes in junctional conductance, via a PSD-mediated mechanism (arrows; Pereda and Faber, 1996; Pereda et al., 1998) promoting the association of CaM-KII to Cx35 and ZO-1. The association of CaM-KII to electrical synapses would be thus non-obligatory and driven by synaptic activity. For convenience, as simplified gap junction is illustrated; the cartoon does not indicate that association is exclusively pre- or postsynaptic.